# JASSA

Journal of Applied Science in Southern Africa
The Journal of the University of Zimbabwe

Volume 2, Number 1, 1996 ISSN 1019–7788


## CONTENTS




**Zimbabwe: Z$30** **Africa: US$15** **Elsewhere: US$20**

# JASSA

*Journal of Applied Science in Southern Africa* **Vol. 2, No. 1, 1996**

**The Journal of the University of Zimbabwe** **ISSN 1019–7788**

## CONTENTS





**Published by University of Zimbabwe Publications**
**P.O. Box MP 203, Mount Pleasant, Harare, Zimbabwe**

**Typeset by University of Zimbabwe Publications**
**Printed by Mazongororo (Pvt.) Ltd., Harare, Zimbabwe**

# Analysis of triaxial test results

D. P. Katale

Department ot Civil Engineering, University of Zimbabwe,
P. O. Box MP 167, Mt Pleasant, Harare, Zimbabwe.

**In order to build a computer-based aid for triaxial results, analysing it is necessary to find ways of putting the human expertise in a computer representation. This paper presents two mathematical approaches to determining the soil shear strength parameters ($c$ and $\varphi$) from triaxial test results. The two resulting sets of equations were tested against each other and they showed very close agreement. In addition to this, they were found to be consistent with published results against which they were also tested. One of the methods produced equations which are simple enough to be used in hand calculations but the other requires the use of a computer.**

**Key words:** soil shear strength, triaxial test, analysis.

The failure state for soils can be represented in many ways (Atkinson and Bransby, 1978; Lamb and Whitman, 1979). Among these is the Mohr-Coulomb failure criterion, one of the most frequently used models for analyses of limiting equilibrium. This failure criterion is described by the equation:

$$\tau = c + \tan\varphi \qquad (1)$$

for the total stress condition, and the equation

$$\tau = c' + \sigma' \tan\varphi = c' + (\sigma - u)\tan\varphi \qquad (2)$$

for the effective stress condition, where $\tau$ = shear strength, $c$ = cohesion, $\sigma$ = normal stress, $\varphi$ = angle of internal friction and $u$ = pore water pressure. The prime (′) is used to indicate effective stress parameters.

The shear strength envelope with respect to total stresses is non linear if observed over a wide cell pressure range. This is because air is being dissolved in the water and later on particles are crushed. But over a limited stress range a linear envelope is adequate. For effective stress conditions, the shear strength envelope approximates to a straight line over a much larger stress range (Bishop and Henkel, 1962).

Soil strength in the field are known to be randomly variable, even for uniform soil layers. As a result, probabilistic model analyses have been suggested as a better means of evaluating the reliability of behaviour predictions made using these statistically variable soil parameters (Chang, 1985 and Andrea and Sangrey, 1982). In order to use these models, the central tendencies and the variability of these values need to be determined.

In the course of developing a computer solution for interpreting laboratory data, it was necessary to describe how a human expert determines the shear strength parameter of a soil from a triaxial test; then translate this knowledge into a computer understandable format.

From triaxial test results and using a method of least squares, this paper develops two methods for determining the shear strength parameters, $c$, $\varphi$, $c'$, $\varphi'$, of equations 1 and 2. A study of the variation of these parameters with the variation in laboratory readings was also made.

## Theory

The shear strength parameters, $c$, $\varphi$, $c'$ and $\varphi'$ describing the Mohr-Coulomb failure criterion in equations 1 and 2 can be measured using a wide variety of methods. Of these, the triaxial test is one of the most commonly used and one of the most versatile testing procedures. The conventional method of analyzing the data from a triaxial test is to draw Mohr circles representing the different stress states at failure of the soil samples, then drawing the best tangent to the circles (see Figure 1).

The angle of this tangent gives the angle of internal friction, φ or φ′, and its intercept gives the cohesion, *c* or *c*′. It should be noted here that the values obtained depend on the skills of the interpreter and that the degree of uncertainty attached to them cannot be quantified. In determining the position of the best tangent, a human expert probably tries to minimize the distance between the circles and the tangent but it is not known for certain that this is true (see Figure 1). In order to give a computer this same capability, the technique of minimizing the sum of squares of the errors was used. The errors considered in this technique were defined in two ways and each of these gave rise to a different procedure.

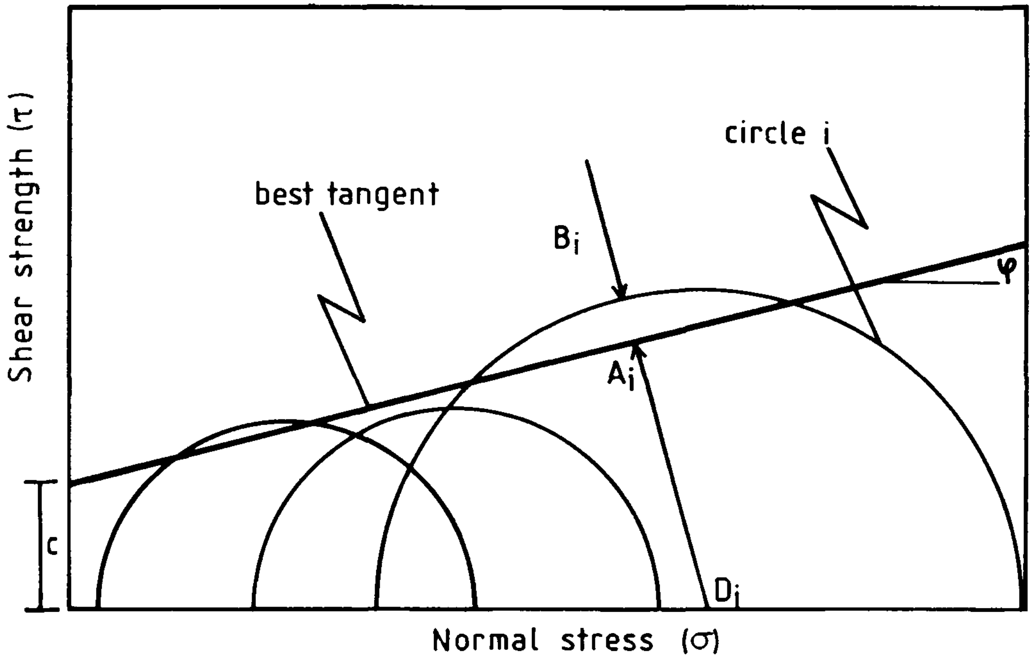

**Figure 1: Typical triaxial test resuts**

*Method 1*

In order to find the total stress parameters, φ and *c*, only the cell pressure, $\sigma_3$, and the deviator stress, $\sigma_1 - \sigma_3$, need to be considered. The cell pressure, $\sigma_3$, is taken as an independent measurement and assumed to have no error. The deviator stress, $\sigma_1 - \sigma_3$, is the dependent variable and carries all the errors inherent in the test procedure. The Mohr-Coulomb failure criterion can be described by the equation:

$$\sigma_1 = \left[\frac{1+\sin\varphi}{1-\sin\varphi}\right]\sigma_3 + 2c\sqrt{\left[\frac{1+\sin\varphi}{1-\sin\varphi}\right]}. \quad (3)$$

Letting ξ be the error in the dependent measurement — that is, the deviator stress and noting that the cell pressure is an independent measurement, equation 3 can be rewritten in the form

$$\sigma_{1i} = \left[\frac{1+\sin\varphi}{1-\sin\varphi}\right]\sigma_{3i} + 2c\sqrt{\left[\frac{1+\sin\varphi}{1-\sin\varphi}\right]} + \xi_i, \quad (4)$$

where

$\sigma_{1i}$ = the major principal stress for the i'th sample,

$\sigma_{3i}$ = the minor principal stress for the i'th sample; also the cell pressure, and

$\xi_i$ = the error in the deviator stress measurement for the i'th sample.

Using the least square model, the sum of squares of the error terms is given by the function

$$S(c,\varphi)=\sum_{i=1}^{n}\xi_i^2=\sum_{i=1}^{n}\left[\sigma_{1i}-\left(\frac{1+\sin\varphi}{1-\sin\varphi}\right)\sigma_{3i}-2c\sqrt{\left(\frac{1+\sin\varphi}{1-\sin\varphi}\right)}\right]^2. \tag{5}$$

This function must be minimized; which implies that

$$\partial S/\partial c=0 \text{ and } \partial S/\partial\varphi=0. \tag{6}$$

Let

$$K_p=\frac{1+\sin\varphi}{1-\sin\varphi}=\tan^2\left(\frac{\pi}{4}+\frac{\varphi}{2}\right). \tag{7}$$

Substituting $K_p$ into equation 5 and differentiating it with respect to $c$ gives

$$\frac{\partial S}{\partial c}=-4\sum_{i=1}^{n}\left(\sigma_{1i}-K_p\sigma_{3i}-2c\sqrt{K_p}\right)\sqrt{K_p} \tag{8}$$

and differentiating with respect to $\varphi$ gives

$$\partial S/\partial\varphi=\left(\partial S/\partial K_p\right)\left(\partial K_p/\partial\varphi\right) \tag{9}$$

Substituting $K_p$ into equation 5 and differentiating it with respect to $K_p$ gives

$$\frac{\partial S}{\partial K_p}=\sum_{i=1}^{n}[-2(\sigma_{1i}-K_p\sigma_{3i}-2c\sqrt{K_p})(\sigma_{3i}+c/\sqrt{K_p})]. \tag{10}$$

Differentiating equation 7 the following expression for $\partial K_p/\partial\varphi$ is obtained:

$$\frac{\partial K_p}{\partial\varphi}=\tan\left(\frac{\pi}{4}+\frac{\varphi}{2}\right)\sec^2\left(\frac{\pi}{4}+\frac{\varphi}{2}\right) \tag{11}$$

$$\frac{\partial K_p}{\partial\varphi}=\tan\left(\frac{\pi}{4}+\frac{\varphi}{2}\right)\left[\tan^2\left(\frac{\pi}{4}+\frac{\varphi}{2}\right)+1\right] \tag{12}$$

$$\frac{\partial K_p}{\partial\varphi}=\sqrt{K_p}(K_p+1). \tag{13}$$

For $\partial S/\partial\varphi$ to be equal to zero, at least one of the following conditions must be true:

$$\partial S/\partial K_p = 0 \tag{14}$$

$$\partial K_p/\partial\varphi = 0 \tag{15}$$

Looking at equations 13 and 7 it can be seen that for the condition of equation 15 to be true, either $K_p = 0$ which is physically impossible or $K_p = -1$ which is both mathematically and physically impossible. This means that only the condition of equation 14 — that is, $\partial S/\partial K_p = 0$ need be used. Inserting equation 8 into equation 6, one finds that

$$-4\sqrt{K_p}\sum_{i=1}^{n}(\sigma_{1i}-K_p\sigma_{3i}-2c\sqrt{K_p})=0. \tag{16}$$

Solving this equation for $c$ one obtains the equation

$$c=(\bar{\sigma}_1-K_p\bar{\sigma}_3)/(2\sqrt{K_p}). \tag{17}$$

where

$$\bar{\sigma}_k=\frac{1}{n}\sum_{i=1}^{n}\sigma_{ki}, \text{ with } k=1 \text{ or } 3. \tag{18}$$

Using equation 10 into equation 14, one obtains the expression

$$\sum_{i=1}^{n}[(\sigma_{1i}-K_p\sigma_{3i}-2c\sqrt{K_p})(\sigma_{3i}+c/\sqrt{K_p})]=0 \tag{19}$$

which can be expanded into

$$\sum_{i=1}^{n}[\sigma_{1i}\sigma_{3i}+c/\sqrt{K_p}\sigma_{1i}-K_p\sigma_3^2-c\sqrt{K_p}\sigma_{3i}-2c\sqrt{K_p}\sigma_{3i}-2c^2]=0. \tag{20}$$

Substituting for $c$ in equation 20 using equation 17 and multiplying through by $K_p$ gives

$$K_p \sum_{i=1}^{n} \sigma_{1i}\sigma_{3i} + \left(\bar{\sigma}_1 - K_p \bar{\sigma}_3\right)$$

$$1/2 \sum_{i=1}^{n} \sigma_{1i} - K_p^2 \sum_{i=1}^{n} \sigma_{3i}^2$$

$$-3K_p(\bar{\sigma}_1 - K_p\bar{\sigma}_3) 1/2 \sum_{i=1}^{n} \sigma_{3i}$$

$$-n(\bar{\sigma}_1 - K_p\bar{\sigma}_3)^2 1/2 = 0. \quad (21)$$

Using equation 14 and collecting the $K_p$ terms, the quadratic equation in $K_p$ shown below is obtained:

$$\left(-\sum_{i=1}^{n} \sigma_{3i}^2 + n\bar{\sigma}_3^2\right) K_p^2$$

$$+\left(\sum_{i=1}^{n} \sigma_{1i}\sigma_{3i} - n\bar{\sigma}_1\bar{\sigma}_3\right) K_p = 0. \quad (22)$$

The only solution to this equation which can have a physical meaning is

$$K_p = \frac{\left(\sum_{i=1}^{n} \sigma_{1i}\sigma_{3i} - n\bar{\sigma}_1\sigma_3\right)}{\left(\sum_{i=1}^{n} \sigma_{3i}^2 \quad - \quad n\bar{\sigma}_3^2\right)} \quad (23)$$

Having determined $K_p$ using equation 23, $c$ is evaluated using equation 17, while φ is determined using equation 7.

For the effective stress analysis, the pore pressure is subtracted from the cell pressure $\sigma_3$ and the axial stress $\sigma_1$ to get $\sigma_3'$ and $\sigma_1'$ respectively. Equations 7, 17, 18 and 23 can then be utilised, but replacing the total stresses $\sigma_3$ and $\sigma_1$ with the effective stresses $\sigma_3'$ and $\sigma_1'$. Thus one can evaluate the effective stress parameters $c'$ and $\varphi'$. It can be deduced here that since the method assumes that the effective cell pressure $\sigma_3'$ is an independent variable, it also implicitly assumes that the pore pressure measurement process does not introduce any errors.

**Method 2**

The second method can be characterised by the intuitive approach of trying to minimize the distances between the circles and the shear strength envelope. Figure 1 shows the distance $e_i$ between the circle *(i)* and the tangent. An error function, $S(c, \varphi)$, is defined as

$$S(c,\varphi) = \sum_{i=1}^{n} e_i^2 \quad (24)$$

The best tangent is then obtained by finding a line which minimizes this function. From Figure 1,

$$e_i = r_i - D_iA_i \quad (25)$$

where $r_i$ = the radius of the circle *(i)* and $D_iA_i$ is the distance from the centre of the circle *(i)* to the shear strength envelope. This shear strength envelope can be represented as

$$\tau = c + \sigma \tan\varphi \ . \quad (26)$$

Let $m = \tan\varphi$ and the centre of the circle *(i)* be at the point $(h_i, 0)$ where $h_i = 1/2(\sigma_{3i} + \sigma_{1i})$, then the distance $D_iA_i$ from the centre of the circle to the envelope is given by

$$D_iA_i = (mh_i + c)/\sqrt{(m^2+1)}\ , \quad (27)$$

(that is, the distance between a point $(h_i, 0)$ and line $\tau = c + m\sigma$). Using equation 25 and 27 to substitute into equation 24, the error function becomes

$$S(c,\varphi) = \sum_{i=1}^{n} e_i^2 =$$

$$\sum_{i=1}^{n}\left(\frac{(mh_i + c)^2}{(m^2+1)} - \frac{2(mh_i + c)r_i}{\sqrt{(m_2+1)}} + r_i^2\right). \quad (28)$$

Minimizing this error function implies that

$$\partial S/\sigma c = 0 \text{ and } \partial S/\partial\varphi = 0. \quad (29)$$

Differentiating equation 28 with respect to $c$ and equating this to zero, one obtains

$$\frac{\partial S}{\partial c} = \sum_{i=1}^{n}\left(\frac{2(mh_i + c)}{m^2+1} - \frac{2r_i}{\sqrt{(m^2+1)}}\right) = 0. \quad (30)$$

$$\Rightarrow \sum_{i=1}^{n}\left(\frac{(mh_i + c)}{\sqrt{(m^2+1)}}\right) - \sum_{i=1}^{n} r_i = 0. \tag{31}$$

After some manipulation, this may be written as

$$c = \frac{1}{n}\left(\sqrt{(m^2+1)}\sum_{i=1}^{n} r_i - \sum_{i=1}^{n} mh_i\right). \tag{32}$$

Taking note of the fact the $m^2 + 1 = \tan^2\varphi + 1 = \sec^2\varphi$ and that the radius $r = 1/2(\sigma_1 - \sigma_3)$, equation 32 can be written as

$$c = \frac{1}{2n}\sum_{i=1}^{n}[\sigma_{1i}(\sec\varphi - \tan\varphi) - \sigma_{3i}(\sec\varphi + \tan\varphi)]. \tag{33}$$

Noting that $m = \tan\varphi$, equation 28 can be written as

$$S(c,\varphi) = \sum_{i=1}^{n}[(h\tan\varphi + c)^2\cos^2\varphi - 2(h\tan\varphi + c)\, r\cos\varphi + r^2]. \tag{34}$$

Differentiating this equation with respect to $\varphi$ and setting it equal zero in order to satisfy the other condition for minimizing the error function, the following equation is derived

$$\begin{aligned}\frac{\partial S}{\partial\varphi} = \sum_{i=1}^{n}[&2(h\tan\varphi + c)h\sec^2\varphi\cos^2\varphi \\ &- (h\tan\varphi + c)^2\cos\varphi\sin\varphi \\ &- 2h\sec^2\varphi\, r\cos\varphi \\ &+ 2(h\tan\varphi + c)\, r\sin\varphi] \\ = 0.&\end{aligned} \tag{35}$$

Further simplification reduces this to

$$\begin{aligned}\frac{\partial S}{\partial\varphi} = \sum_{i=1}^{n}[&(h\tan\varphi + c) - (h\tan\varphi + c)^2 \\ &\cos\varphi\sin\varphi - h\, r\sec\varphi \\ &+ (h\tan\varphi + c)\, r\sin\varphi] \\ = 0 = R(c,\varphi)&\end{aligned} \tag{36}$$

$R(c, \varphi)$ is a residual function introduced here and will be used to find a solution indirectly. Two equations with two unknowns, $c$ and $\varphi$, have been derived, therefore their values can be evaluated. The equations are, however, too complicated for a direct solution. A binary search strategy was adopted to accomplish this.

It is known that the friction angle of a soil must lie in the interval 0–90°. The binary search method works by dividing the interval into two equal halves and then identifying the half in which the target solution is located. This gives a smaller interval by which one is sure of finding the solution. The procedure is repeatedly carried out until the target interval is small enough for the required purpose. It should be emphasised here that the method only gives an interval within which the solution is known to lie.

In order to identify this interval, the following procedure has been adopted. Values of $\varphi$ at the two ends of the intervals, $\varphi_L$ for the left side and $\varphi_R$ for the right, plus one value, $\varphi_C$, at the centre are used in equation 33 to determine three values of $c$. These values are in turn used in equation 36 to determine three residual values of $R(c,\varphi)$ corresponding to the three $\varphi$ values used (see Figure 2).

The sub-interval within which the target solution lies is the one whose bounding residuals have opposite signs. For example, in Figure 2 the interval $\varphi_L$ to $\varphi_C$ is the relevant interval. This procedure is repeated until the required accuracy is obtained. It is also possible in a rare event to have a residual equal to zero, in which case the corresponding $\varphi$ value represents the solution and no further search need be made. The number of iterations needed to locate the interval is constant for a required accuracy and, at most, is $(1 + \log_2 (90°/A)$ truncated to an integer. $A$ is the required accuracy. For example, to get a target interval no greater than 0,1°, at most ten iterations would be required. It should be noted that the values of the residual at the end are not important and do not affect the accuracy of the friction angle and the cohesion obtained.

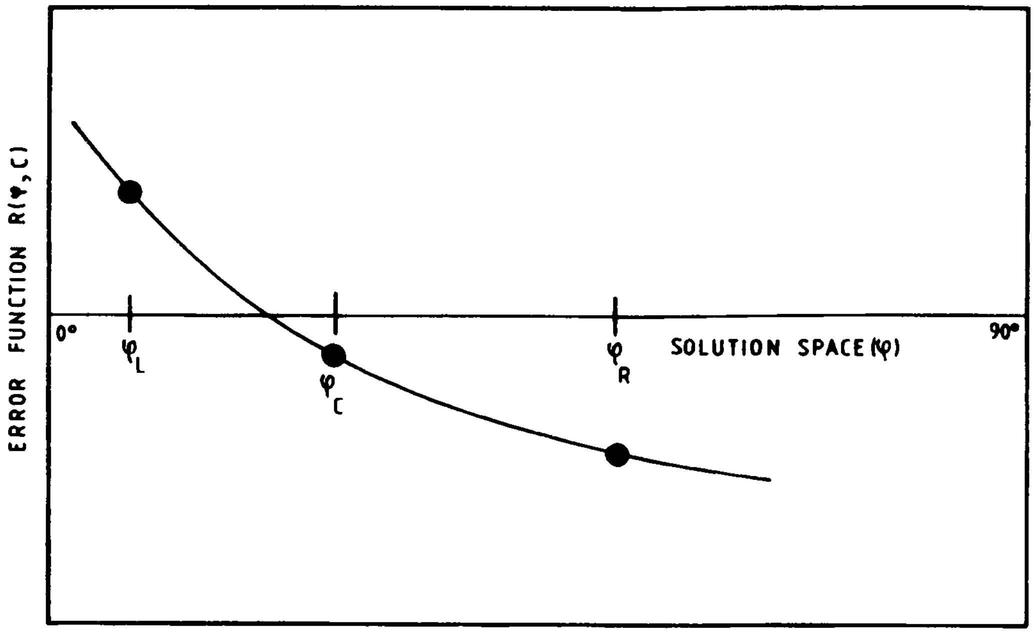


**Figure 2: A binary search iteration**

Procedures in the "BASIC" language were written to utilise the two derived methods.

## DISCUSSION AND RESULTS

Results published by Akroyd (1957), de Graft *et al.* (1969), de Castro (1978), Scott (1980), Smith (1982) and Geotechnical Control Office (1984), together with the cohesion and friction angles obtained in their analyses, were used for comparison. In order to assess the validity of the two methods, 1 and 2, the shear strength parameters from the derived equation were compared with those of the conventional method. Figures 3 and 4 show the cohesion obtained using methods 1 and 2 respectively, against the conventional methods, while Figures 6 and 7 represent the comparison of the two methods with respect to the friction angle.

The regression lines drawn through the points in all the four cases are very close to the 45° lines which are also shown on the graphs as broken lines. It can, therefore, be concluded that both methods can reliably be used to determine $c$ and $\varphi$. In addition to this, it can be noted that there was some scatter of the points about the regression lines. This gives an indication of the differences caused by the judgement of the various individuals who obtained the values of $c$ and $\varphi$ using the conventional method. This kind of variation would be eliminated by employing the derived methods. Figures 5 and 8 show a comparison of the two methods against each other.

It was found that the two methods gave the same results to the first decimal point and produced a 45° line with virtually no discernable scatter. The equations derived in method 1 have a simplicity which made it possible to write a short and quick computer algorithm and indeed they are simple enough to be used in hand calculations. The derivation of the second approach, on the other hand, has an intuitive feel but the resulting equations are more complicated and not easily handled by hand calculations. In addition, the algorithm written to handle these equations was found to be both long and slow. Both methods enable the analysis of triaxial test results to be handled by computers.

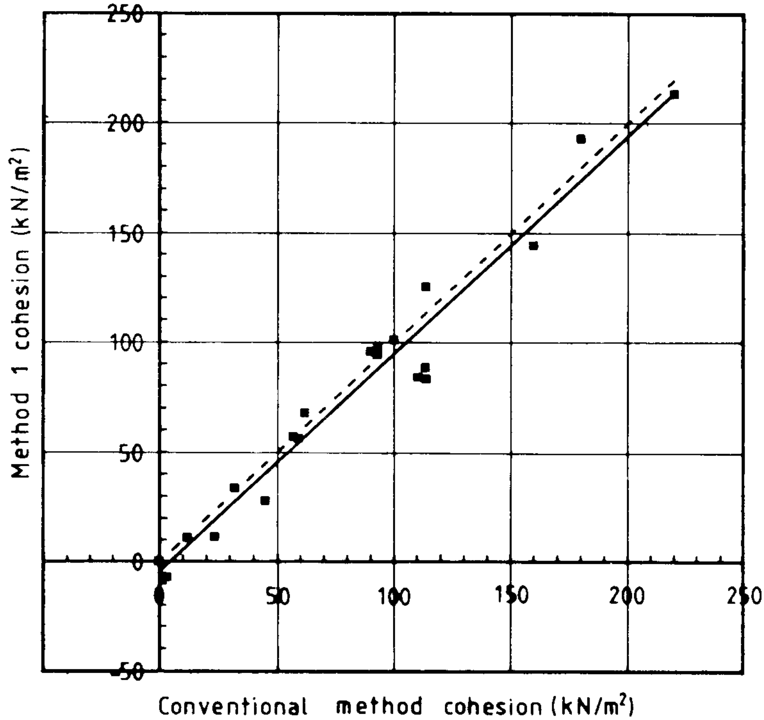


**Figure 3:** Method 1 vs conventional method (cohesion)

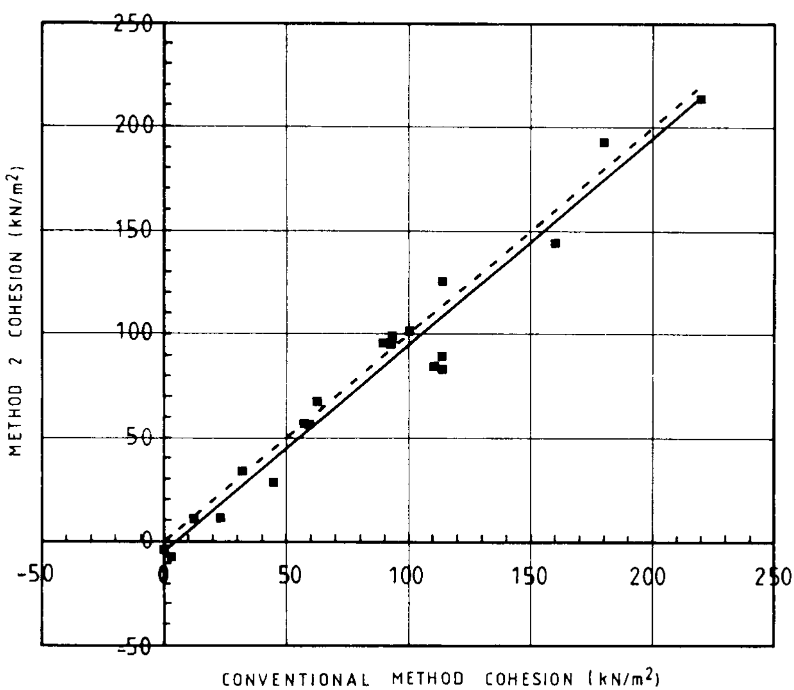


**Figure 4:** Method 2 vs conventional method (cohesion)

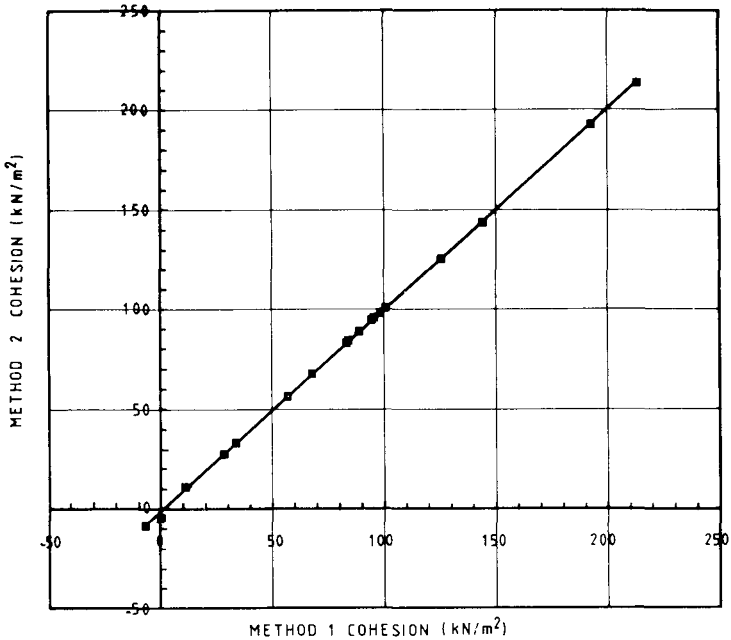


Figure 5: Method 2 vs method 1 (cohesion)

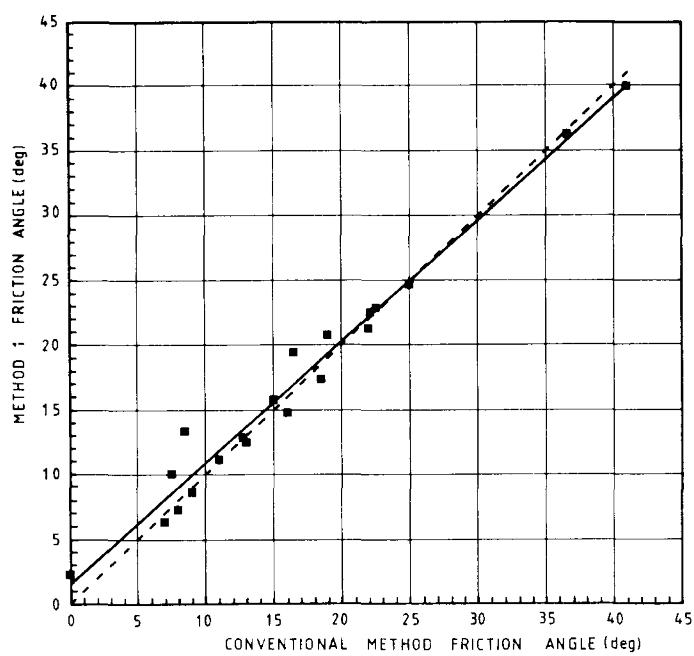


Figure 6: Method 1 vs conventional method (friction angle)

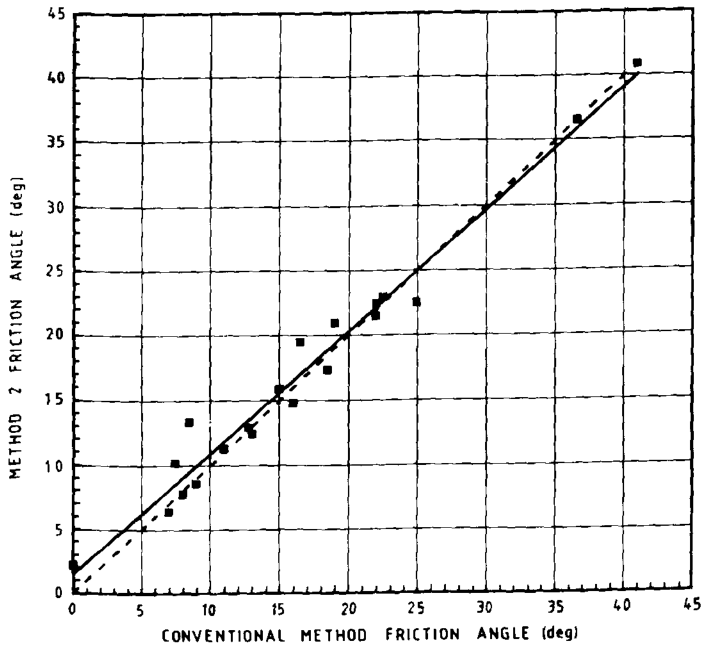


**Figure 7: Method 2 vs conventional method (friction angle)**

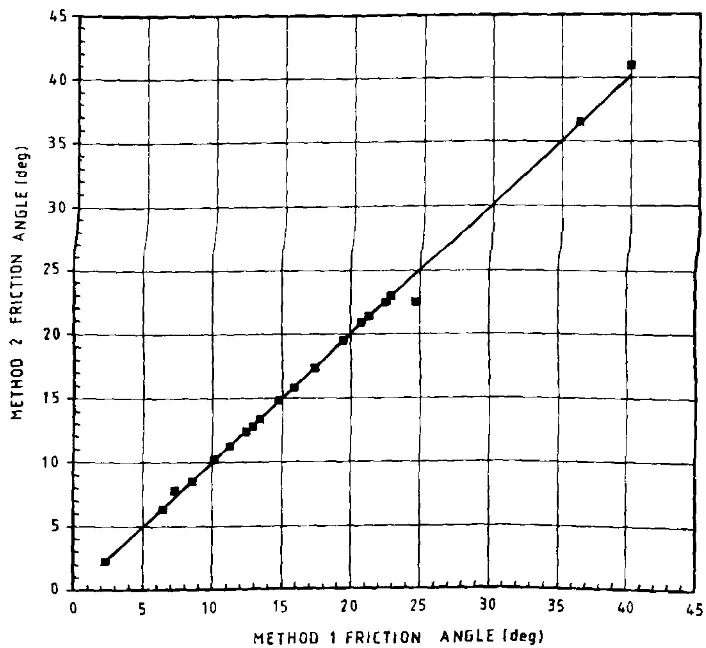


**Figure 8: Method 2 vs method 1 (friction angle)**

## CONCLUSION

Two methods for the analysis of triaxial test results have been proposed. The methods can both be used on a computer. In addition, the simplicity of the first method allows it to be used without too much difficulty in hand calculations.

The two methods give the same results as the conventional method and with less subjectivity.

Although both methods give similar results, method 1 is preferred to method 2 because it is simple.

## NOTATION

The following symbols are used in this paper:

| | | |
|---|---|---|
| A | = | the required accuracy in a binary search |
| $e_i$ | = | the distance between the shear strength envelope and the i'th circle |
| h | = | $1/2(\sigma_1 + \sigma_3)$ — that is, the centre of Mohr's circle of stresses. |
| i, k | = | indices |
| $K_p$ | = | a constant introduced in equation 7 = $(1+\sin\varphi)/(1-\sin\varphi)$ |
| m | = | $\tan\varphi$ |
| n | = | number of samples tested in a single triaxial test |
| r | = | radius of Mohr's circle of stresses = $1/2(\sigma_1 - \sigma_3)$ |
| $R(c, \varphi)$ | = | residual function introduced in equation 36 |
| $\varphi$ | = | the friction angle of the soil |
| $\varphi_{L}$, $_{C}$, and$_{R}$ | = | friction angles on the left, at the centre and on the right of a search interval. |
| $\sigma_1, \sigma_3$ | = | the cell and vertical pressure (major and minor principle stresses) |
| $\tau$ | = | the shear stress |
| $\xi_i$ | = | the error in the deviator stress for the i'th sample |

## REFERENCES


Akroyd, T.N.W. 1957 Laboratory testing in Soil Engineering. Soil Mechanics Ltd.

Atkinson, J.H. and Bransby, P.L. 1978 The Mechanics of soils — *an introduction to critical state soil mechanics*, McGraw-Hill, London.

Bishop, A.W. and Henkel, D.J. 1962 The measurement of soil properties in the triaxial test, Edward Arnold.

Chang, Ching S., 1985 "Uncertainty of One-Dimensional Consolidation Analysis" Journal of the Goetechnical Engineering Division, ASCE 3, No. 12: 1411.

D'Andrea, R.A. and Sangrey, D.A. 1982 "Safety Factors for Probabilistic Slope Design," *Journal of the Geotechnical Engineering Division*, ASCE 108 (GT9): 1101.

De Castro, Lydia, C. 1978 "Strain Rate Influence on Shear Strength Characteristics of Compacted Fadama Clays," Ph.D. Thesis, ABU.

De Graft Johnson, J.W.S., Bhatia, H.S. and Gidigasu, D.M. 1969 "The strength Characteristics of Residual Micaceous Soils and their Applications to stability problems," Proceedings. of the 7th. International Conference *on Soil Mechanics and Foundation Eng*ineering, Session 1, pp.165.

Geotechnical Control Office, 1984 *Geotechnical Manual for Slopes* (2nd ed.), Engineering Development Department. Government of Hong Kong.

Lamb, T. Williams and Whitman, Robert, V. 1979 *Soil Mechanics*, SI Version, John Wiley and Sons.

Scott C.R. 1980 *An Introduction to Soil Mechanics and Foundations* (3rd ed.) Applied Science Publishers Ltd.

Smith, G.N. 1982 *Elements of Soil Mechanics for Civil and Mining Engineers* (5th ed.) Collins Professional Books.